

RuvB Protein-Mediated ATP Hydrolysis: Functional Asymmetry in the RuvB Hexamer[†]

Paul E. Marrione and Michael M. Cox*

Department of Biochemistry, College of Agriculture and Life Sciences, University of Wisconsin, Madison, Wisconsin 53706

Received February 23, 1995; Revised Manuscript Received May 19, 1995*

ABSTRACT: A survey of RuvB protein-mediated ATP hydrolysis yields the following observations. (1) The RuvB protein exhibits a DNA-independent ATPase activity with a turnover number (based on a RuvB monomer) approaching 6 min⁻¹ and a K_m of 154 μ M. Single-stranded DNA and linear duplex DNA have small but significant effects on this activity. (2) At ATP concentrations near the K_m , the ATPase activity is attenuated after ~ 60 turnovers/RuvB monomer. The attenuation does not reflect inhibition by ADP. Addition of ATP to 3 mM triggers an immediate resumption of ATP hydrolysis. The attenuation is enhanced somewhat by ssDNA and reduced somewhat by linear dsDNA. (3) ATP hydrolysis is dramatically stimulated by circular dsDNA, reinforcing the notion that RuvB translocates along the DNA in a reaction coupled to ATP hydrolysis. The k_{cat} increases by at least 2–4-fold on circular duplexes depending on conditions, and the inactivation of RuvB at ATP concentrations near the K_m does not occur. The ATPase activity on circular dsDNA also exhibits a partial substrate inhibition by ATP. (4) Optimal ATP hydrolysis requires ~ 1 DNA circle/RuvB hexamer, suggesting that multiple RuvB hexamers on a circle have an inhibitory effect on the ATPase activity. (5) With or without any of these DNA cofactors, a burst of ATP hydrolysis is observed under pre-steady-state conditions equivalent to 1 ATP per 3–3.3 RuvB monomers (2 ATP/hexamer). The substrate inhibition and burst results suggest the presence of nonequivalent ATP hydrolytic sites in a RuvB hexamer. The attenuation of ATPase activity observed under some conditions may also be a manifestation of nonequivalent ATP hydrolytic sites.

The RuvA and RuvB proteins of *Escherichia coli* function at a late stage of recombinational DNA repair and homologous genetic recombination to process branched DNA intermediates created by the action of RecA protein (Shinagawa et al., 1991; West & Connolly, 1992; West et al., 1993; Kuzminov, 1993; Müller & West, 1994; Kowalczykowski et al., 1994). In vitro, these proteins promote a rapid branch migration of Holliday junctions (Lloyd & Sharples, 1993; Tsaneva et al., 1992b) and possess a DNA helicase activity (Tsaneva et al., 1993; Tsaneva & West, 1994). When RecA protein-mediated DNA strand exchange is blocked by heterologous DNA sequences in one of the DNA substrates, RuvA and -B facilitate either a bypass of the barrier or the reversal of the strand exchange reaction (Iype et al., 1994, 1995). The helicase activity is believed to be mechanistically related to the promotion of branch migration and the processing of branched DNA molecules in which branch migration is blocked (Müller & West, 1994; Tsaneva & West, 1994; Iype et al., 1995). The helicase and branch migration activities are both dependent on the hydrolysis of ATP by RuvB protein. The RuvA protein facilitates the binding of RuvB protein to DNA and is required for helicase function. The primary structure of the RuvB protein features at least one consensus ATP-binding fold (Benson et al., 1988; Shinagawa et al., 1988).

DNA helicases must translocate as they unwind DNA, and both the translocation and DNA unwinding are somehow coupled to the hydrolysis of ATP. There are at least two structural classes of helicases. Proteins such as the SV40 T

antigen (Dean et al., 1992; Dean & Hurwitz, 1991), the Rho protein (Geiselman et al., 1992a–c; Geiselman et al., 1993; Seifried et al., 1992; Wang & von Hippel, 1993), and the DnaB protein (Bujalowski et al., 1994) function as hexamers. In contrast, the Rep protein and DNA helicase III are active as dimers (Lohman, 1992, 1993; Wong et al., 1992; Wong & Lohman, 1992). The RuvB protein appears to function as a hexamer, with a dodecameric species observed under some conditions reported to be inactive (Mitchell & West, 1994; Stasiak et al., 1994).

The ATPase activity of RuvB was first examined by Shinagawa and co-workers (Iwasaki et al., 1989), who observed a low ATP turnover rate and an apparent substrate or product inhibition in the absence of DNA. More recent characterization by West and colleagues (Mitchell & West, 1994) has provided evidence for a stimulation of ATP hydrolysis by dsDNA, with the greatest stimulation occurring when the DNA was circular. The RuvB ATPase is also stimulated by RuvA protein (Mitchell & West, 1994). In this report, we build on these observations and survey the ATP hydrolytic activity of RuvB alone, using both steady-state and pre-steady-state approaches. The results provide new evidence that RuvB protein translocates along dsDNA and reveal a functional asymmetry among the ATP hydrolytic sites of a RuvB hexamer.

MATERIALS AND METHODS

Reagents, Buffers, and RuvB Protein. *Escherichia coli* RuvB protein was purified and stored as described previously (Iype et al., 1994; Tsaneva et al., 1992a). The final yield of

[†] P.E.M. was supported by NIH Predoctoral Training Grant GM07215.

* Abstract published in *Advance ACS Abstracts*, July 15, 1995.

RuvB protein from 13 g of cells was 27 mg. The RuvB protein was >95% pure as determined by Coomassie-stained SDS¹-PAGE gels and was free from detectable endo- or exonuclease activities. The concentration of RuvB protein was determined spectrophotometrically at 280 nm using $\epsilon_{280,\text{native}} = 1.64 \times 10^4 \text{ M}^{-1} \text{ cm}^{-1}$ (determined as described below). Freezing and thawing the protein preparations twice had no detectable effect on the steady-state kinetic parameters for ATP hydrolysis. On the basis of the consistent specific activities of the multiple preparations of RuvB generated over the past year, and the absence of significant activity losses upon storage for several weeks on ice, we assume that the RuvB protein is 100% active.

Molecular biology grade Tris buffer and Spectroscopy grade glycerol was obtained from Fisher Scientific. Pyruvate kinase, lactate dehydrogenase, reduced β -nicotinamide adenine dinucleotide (NADH), phosphoenolpyruvate (PEP), bovine serum albumin (BSA), adenosine 5'-triphosphate (ATP), ultrapure guanidine hydrochloride, and all molecular biology grade salts were from Sigma Chemical Co. The purity of ATP from Sigma was checked by thin-layer chromatography (see below) and was shown to be at least 99% pure, with the major contaminant being ADP. The concentration of ATP was determined by absorbance at 259 nm, using the extinction coefficient $\epsilon_{259} = 1.54 \times 10^4 \text{ M}^{-1} \text{ cm}^{-1}$. [α -³²P]ATP (3000 Ci/mmol) was from Amersham. Labeled ATP with greater than 5% ADP contamination was not used in experiments. Machery-Nagel polyethylenimine cellulose (PEI-cellulose) thin-layer chromatography (PEI/UV₂₅₄) sheets were purchased from Brinkmann. Restriction enzymes were from New England Biolabs, and topoisomerase I was from Gibco-BRL.

The following buffers were prepared with deionized double-distilled water. Buffer A, used for measurement of the RuvB extinction coefficient, was 20 mM Tris-HCl (78% cation), 12.6% (w/v) glycerol, 0.15 M NaCl, 1 mM Na₃-EDTA, and 0.5 mM dithiothreitol. The final pH of buffer A was 7.55 at room temperature. Solutions of 6 M guanidine hydrochloride were dissolved in 20 mM Tris-HCl (78% cation, pH 7.6), 0.15 M NaCl, 1 mM Na₃EDTA, and 0.5 mM dithiothreitol. Buffer B, used in the experiments measuring the RuvB ATP hydrolytic activity, was 20 mM Tris acetate (80% cation), 15 mM magnesium acetate, 6.3% (w/v) glycerol, 3 mM potassium glutamate, 2 mM dithiothreitol, and 100 $\mu\text{g}/\text{mL}$ BSA. The final pH of buffer B was 7.65 at room temperature. RuvAB dilution buffer contained 20 mM Tris acetate (80% cation), 0.15 M NaCl, 12.6% (w/v) glycerol, 1 mM Na₃EDTA, 0.5 mM dithiothreitol, and 100 $\mu\text{g}/\text{mL}$ BSA. The final pH of the dilution buffer after addition of all components was 7.65.

DNA Substrates. Circular single-stranded DNA from bacteriophage M13mp8 and supercoiled circular duplex pJFS35r DNAs were prepared using methods described previously (Davis et al., 1980; Messing, 1983; Neuendorf & Cox, 1986). The pJFS35r plasmid was over 95% supercoiled as determined by densitometric scanning of agarose gels (data not shown). The plasmid pJFS35r is a 2820 bp plasmid derived from the plasmid pXF3, containing a copy of the recombination target site recognized by the

yeast FLP recombinase inserted between the *Eco*RI and *Bam*HI sites (Senecoff & Cox, 1986). The concentrations of ssDNA and dsDNA were determined by absorbance at 260 nm, using 36 and 50 $\mu\text{g mL}^{-1} A_{260}^{-1}$, respectively, as the conversion factors. DNA concentrations are reported in terms of total nucleotides.

Full-length linear single-strand DNA was derived from the circular single-strand DNA of M13mp8 by annealing an 18 bp synthetic oligonucleotide (University of Wisconsin Biotechnology Facility) spanning the *Eco*RI recognition site and digesting to completion with the restriction endonuclease *Eco*RI. Full-length linear duplex DNA was obtained by digesting the plasmid pJFS35r with the restriction endonuclease *Pst*I. Relaxed pJFS35r plasmid DNA was prepared from the supercoiled circular duplex plasmid pJFS35r by incubation with topoisomerase I. All restriction enzyme digestions were performed as recommended by the enzyme supplier. To purify DNAs following enzyme treatments, reaction mixtures were extracted sequentially with phenol/chloroform/isoamyl alcohol (25:24:1) and chloroform/isoamyl alcohol (24:1), followed by ethanol precipitation.

Determination of the Extinction Coefficient for RuvB Protein. The determination of the extinction coefficient for native RuvB protein is based on a modification of a published procedure (Lohman et al., 1989). UV absorbance spectra were measured using a Perkin-Elmer Lambda 7 double-beam recording spectrophotometer. Temperature was maintained with a circulating water bath. Cell path length and band width were 0.5 cm and 2 nm, respectively. The extinction coefficient for native RuvB protein was determined in buffer A by comparing the absorbance spectra of the native protein to the absorbance spectra of the protein denatured in 6 M guanidine hydrochloride (Gdn-HCl). The extinction coefficients for glycyl-L-tyrosylglycine and *N*-acetyl-L-tryptophanamide are 1280 and 5690 $\text{M}^{-1} \text{ cm}^{-1}$, respectively (Edelhoch, 1948). In the RuvB polypeptide, there are seven tyrosines, one tryptophan, and no cysteines. The extinction coefficient of the RuvB protein in 6 M Gdn-HCl is calculated as $\epsilon_{280}(6 \text{ M Gdn-HCl}) = 1(5690) + 7(1280) = 1.47 \times 10^4 \text{ M}^{-1} \text{ cm}^{-1}$. Absorbance spectra of native and denatured (6 M Gdn-HCl) protein were scanned at 25 °C, from 320 to 240 nm, at six different dilutions of stock protein and with two different protein preparations. The concentrations of native and denatured protein were equal to each other in each scan at each dilution. The extinction coefficient of the native RuvB protein was determined at 280 nm according to the expression (Gill & von Hippel, 1989)

$$\epsilon_{280,\text{M,nat}} = [(\text{Abs}_{\text{nat},280})(\epsilon_{\text{M},280;6\text{MGdn-HCl}})]/\text{Abs}_{\text{Gdn-HCl},280}$$

Six determinations on two different preparations of RuvB protein yielded an average extinction coefficient of $\epsilon_{280} = (1.64 \pm 0.06) \times 10^4 \text{ M}^{-1} \text{ cm}^{-1}$ in buffer A at 25 °C. The absorbance maxima for the native and denatured proteins is 270 nm. The A_{280}/A_{260} ratio for the native RuvB protein is 0.94 ± 0.06 . We attribute this to the single tryptophan in RuvB (about one-third the number expected on average for a 306 amino acid protein), so that the tyrosine residues (seven) and perhaps the phenylalanine residues make a larger than normal contribution to the absorbance spectrum.

Assays To Measure ATP Hydrolysis. The coupled spectrophotometric assay used to measure ATP hydrolysis, employing pyruvate kinase and lactate dehydrogenase, was

¹ Abbreviations: ssDNA, single-stranded DNA; dsDNA, double-stranded DNA; SDS, sodium dodecyl sulfate; bp, base pair(s), kbp, kilobase pairs; Gdn, guanidine.

described previously (Morrical et al., 1986; Lindsley & Cox, 1990; Iype et al., 1994). Kinetic effects described in the text affected the useful time period over which data could be collected in some experiments. When the ATP concentration was 125 μ M in experiments with no DNA, and with ssDNA or linear dsDNA, initial rates were derived from data collected in the first 10 min of reaction (at later times the rates were attenuated). In reactions in which circular dsDNA was used as a DNA cofactor, reported reaction rates were derived from data collected between 20 and 60 min after initiation of reaction (an extended lag was evident at earlier times).

Reactions were carried out at 37 °C in buffer B containing 1.93 mM NADH, an ATP regeneration system (2.94 units/mL pyruvate kinase and 2.48 mM PEP), and 2.94 units/mL lactate dehydrogenase, in a reaction volume of 400 μ L. Reactions were preincubated for 10 min at 37 °C with all components except RuvB and initiated by addition of the RuvB protein. All reactions were carried out with 1.05 μ M RuvB protein unless noted, and various types of DNA were included in some reactions as indicated in figure legends and Results. After addition of all reaction components, the final pH of the reaction mixtures was 7.65 at room temperature. Rates obtained with the coupled spectrophotometric assay were in agreement with rates obtained by the thin-layer chromatography assay described below (data not shown). Mitchell and West (1994) have reported that RuvB is in a hexameric form in a buffer essentially equivalent to buffer B with 1 mM ATP. We assume that a hexameric species is the predominant form of RuvB in the experiments described below.

In some assays, the effect of adding additional ATP or supercoiled DNA to an ongoing ATPase assay was investigated. In these experiments, two reactions (400 μ L each) at a substrate concentration of 125 μ M ATP were initiated by the addition of RuvB protein. These reactions were monitored for 30 min. At 30 min, the concentration of ATP in one reaction was increased to 3 mM by the addition of 20 μ L of a prewarmed concentrated ATP stock solution in buffer B (or, alternatively, supercoiled pJFS35r plasmid DNA was added to a final concentration of 100 μ M nucleotides in buffer B + 125 μ M ATP). The control reactions in either case received a 20 μ L aliquot of 125 μ M ATP in buffer B. After the addition of the ATP, the reactions were monitored for an additional 35 min. As a control to account for the dilution effect of the added volume of ATP, a set of reactions at 1 mM ATP were run in parallel. One of these reactions received ATP to 3 mM (or supercoiled plasmid pJFS35r to 100 μ M in buffer B + 1 mM ATP) and the other in either case received an aliquot of 1 mM ATP in buffer B. The dilution of RuvB protein after addition of the ATP was taken into account in calculating reaction rates.

In this system, the spectrophotometric assay above reliably monitors ATP hydrolytic reactions to 125 μ M ATP. A thin-layer chromatography (TLC) assay was used to measure ATP hydrolysis rates at ATP concentrations below 125 μ M. The PEI-cellulose TLC plates were developed in water until the solvent front reached the top of the plate, and the plate was permitted to overdevelop (solvent continuously running up the plate) overnight. The plates were dried and stored at 4 °C. This step is necessary to clean the plates for more efficient separations as instructed by the manufacturer. ATPase reaction conditions were identical to those using the

coupled assay above except that the ATP regeneration system was omitted, and [α - 32 P]ATP was added to monitor hydrolysis. The reaction volume was 100 μ L. As before, the reactions were preincubated for 10 min at 37 °C and started by the addition of RuvB protein. Aliquots (1 μ L) of the reaction were spotted at various time points to the prewashed TLC plates to quench the hydrolysis reactions. The TLC plates were developed in 1 M formic acid/0.5 M LiCl. The plates were dried and exposed to storage phosphor screens (Molecular Dynamics). The exposed phosphor screens were scanned with a Molecular Dynamics PhosphorImager (Model 425E). The radioactivity in the ATP and ADP spots was quantified using ImageQuaNT software, and the percent ATP hydrolyzed was calculated and plotted versus time. The percent ATP hydrolyzed per minute was calculated by a linear least-squares fit to all data points obtained before 10% of the substrate was consumed in the reaction. The rate of ATP hydrolysis was calculated with the expression

$$\text{ATPase rate} = ([\text{percent ATP hydrolyzed/min}] \times [\text{ATP}]_0) / 100$$

where $[\text{ATP}]_0$ is the concentration of ATP at time zero (before addition of RuvB protein). Assays were repeated on different days.

The TLC assay was also used for the analysis of burst kinetics in RuvB-mediated ATP hydrolysis. Reaction conditions are described in figure legends and Results. Reactions were preincubated for 10 min at 37 °C, and RuvB protein was added and mixed thoroughly to initiate the reaction. Total reaction volume was 100 μ L, and immediately after mixing, aliquots (1 μ L) were removed and spotted onto TLC plates every 5 s up 50 s, then every 10 s to 1.5 min, then every 15 s to 2.5 min, and then every 30 s to 5 min (23 aliquots total). To determine the background level of ADP, an aliquot was removed in duplicate at time zero (before addition of RuvB protein). The TLC plates were developed and quantified as described above. The linear portion of the curve was fitted by linear least squares (correlation coefficients >0.98). These lines were extrapolated to zero time to obtain the percentage of ATP at the burst. The size of the burst was calculated with the following equation.

$$\text{burst } (\mu\text{M ATP}) = \{[(\text{extrapolated } Y \text{ intercept}) - (\text{background ADP})] \times [\text{ATP}]_0\} / (100 - \text{background ADP})$$

where $[\text{ATP}]_0$ is the concentration of ATP in the reaction as described in the figure legends. The burst size was plotted versus concentration of RuvB protein and the number of RuvB monomers per 1 ATP was calculated for each concentration of RuvB protein. The results are the mean of eight experiments at four different protein concentrations with the error reported as the standard error of the mean.

As a control to ensure that reactions are efficiently stopped when spotted onto the PEI-cellulose TLC plates, a pair of identical ATPase reactions were carried out side by side. Timed aliquots from one were treated as described above, while the aliquots from the other were stopped by addition to 10% HClO₄ prior to spotting on the TLC plates as described (Moore & Lohman, 1994). The two methods yielded identical results (data not shown).

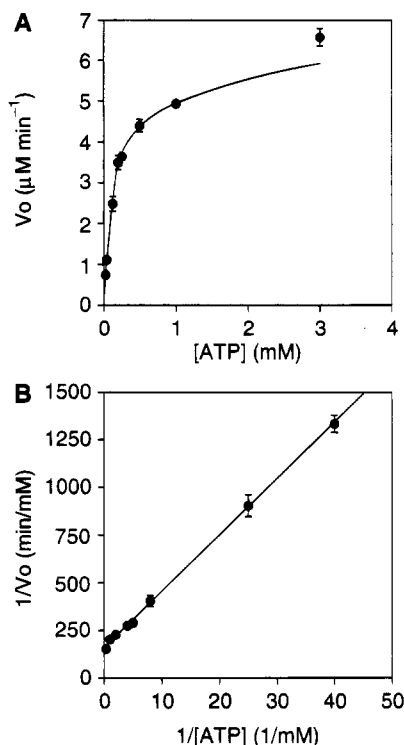


FIGURE 1: Steady-state kinetic analysis of RuvB-mediated ATP hydrolysis in the absence of DNA. Reactions were carried out as described in Materials and Methods. Assays contained 1.05 μM RuvB protein (monomers) and covered a range of substrate concentration from 25 μM to 3 mM ATP. The data for 125 μM to 3 mM ATP were obtained with the coupled spectrophotometric ATPase assay, and the initial velocities of ATP hydrolysis at 25 μM and 50 μM ATP were obtained with the TLC assay. Each data point is the average of three experiments performed on different days, and the error bars represent the range of data obtained.

Kinetic Data Analysis. Initial velocities of reactions (v_0) were analyzed using the program HYPER (Cleland, 1979a). This program fits initial reaction velocities to the Michaelis–Menten equation: $v_0 = (V_{\max}[S])/(K_m + [S])$ by the least-squares method for the reciprocal plots. The assumptions in this program are that the errors in data reside in the experimental parameter (velocities or kinetic constants derived from velocities) and that the errors are random. In other words, the errors in substrate or cofactor concentration are negligible compared to errors in the experimental parameters. In addition, the magnitude of the initial rates over the total range of substrate concentrations examined varied by less than a factor of 5, and analysis of the data showed the errors to be random (data not shown). In experiments where repetitions were performed, each repetition was analyzed separately with HYPER. The values reported are the average of the independent determinations, and the error is the standard error of the experimental parameter.

RESULTS

RuvB Protein-Mediated ATP Hydrolysis in the Absence of Added DNA. A number of experiments were carried out to define standard reaction conditions. Initial rates of ATP hydrolysis by RuvB protein are shown in Figure 1. The RuvB protein obeys Michaelis–Menten kinetics in the range of ATP concentration from 25 μM to 1 mM ATP. As the substrate ATP concentration increases, the initial velocity

Table 1: Summary of Derived Steady State Rate Constants for RuvB Protein-Mediated ATP Hydrolysis^a

DNA	derived K_m (μM ATP)	derived k_{cat} (min^{-1})
none	154 ± 13	5.50 ± 0.17
circ ssDNA	145 ± 14	5.87 ± 0.19
lin ssDNA	121 ± 10	5.67 ± 0.14
lin dsDNA	81 ± 9	6.76 ± 0.17

^a All reactions contained 1.05 μM RuvB protein. Procedures and programs used for data analysis are described in Methods. DNA concentrations are 100 μM except where indicated. The ssDNA substrates were derived from M13mp8, and the dsDNA substrates were from the plasmid pJFS35r.

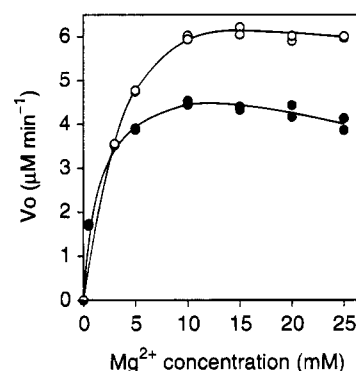


FIGURE 2: Effects of Mg^{2+} on RuvB protein-mediated ATP hydrolysis. All rates were obtained with the spectrophotometric assay, and carried out as described in Materials and Methods. Reactions contained 1.05 μM RuvB protein and either 0.5 (●) or 3.0 mM ATP (○).

of the ATP hydrolysis reaction increases hyperbolically. However, a slightly higher than expected rate was obtained as a substrate concentration of 3 mM ATP. This higher rate suggests a low level of negative cooperativity in the ATPase activity at higher ATP concentrations. These data provide a K_m value for ATP of 154 ± 13 μM ATP and a k_{cat} of 5.50 ± 0.17 min^{-1} (see Table 1). In analyzing these data with HYPER, the rates obtained at 3 mM ATP were not included because of the apparent negative cooperativity.

The effect of magnesium concentration on the RuvB ATPase at substrate concentrations of 0.5 and 3 mM ATP is shown in Figure 2. The ATPase activity of RuvB reaches a maximum at concentrations above 10 mM magnesium ions. At magnesium concentrations equal to the ATP concentration (i.e., 0.5 mM magnesium with 0.5 mM ATP and 3 mM magnesium with 3 mM ATP), the observed rate of ATP hydrolysis is 40% and 60%, the maximum values at 0.5 mM and 3 mM ATP, respectively. A magnesium concentration of 15 mM was adopted as standard and used in further experiments. We note that there is a slight inhibition of the ATPase activity with 0.5 mM ATP at the higher magnesium concentrations. The apparent negative cooperativity seen in Figure 1 might reflect the relief of a low level of magnesium inhibition as higher levels of ATP titrate out the free magnesium. This possibility was not investigated in detail.

The effect of varying RuvB promoter concentration on the rates of ATP hydrolysis is shown in Figure 3. These data show that an apparent critical concentration of RuvB protein monomers, in the range of 200 nM, must be exceeded before the RuvB protein complex can hydrolyze ATP. Below 200 nM RuvB monomers, no ATPase activity was detected. At 260 nM RuvB monomers, a low-level ATPase activity was present, but the turnover at ATP was only 2.3

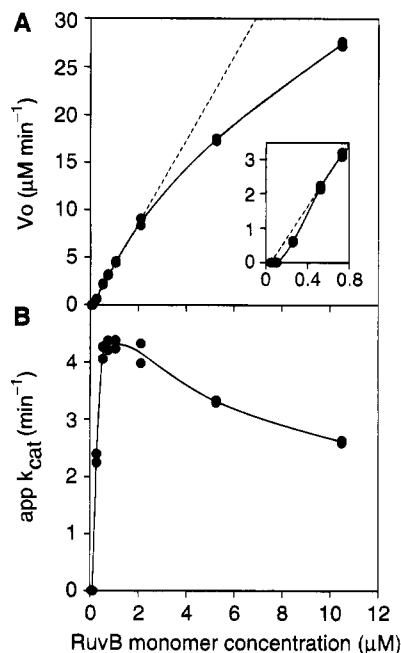


FIGURE 3: Dependence of RuvB-mediated and DNA-independent ATP hydrolysis on RuvB protein concentration. All reactions contained 1 mM ATP and no DNA. At low concentrations of RuvB protein, the protein was diluted into RuvAB dilution buffer as needed. Initial rates are plotted in panel A, with the data obtained at low RuvB protein concentrations expanded in the inset. In panel B, the data in panel A is divided by the concentration of RuvB protein to yield an apparent k_{cat} .

min^{-1} . The rate of ATP hydrolysis exhibits a linear dependence on RuvB concentration from 525 nM to 2.1 μM RuvB promoters, and in this range the turnover of ATP is constant at 4.2 min^{-1} . Above 5.25 μM RuvB protein, the rate of ATP turnover declines. A concentration of 1.05 μM RuvB protein monomers, in the linear region of the protein titration curve, is used in the remaining experiments.

Effects of ssDNA and Linear dsDNA on RuvB-Mediated ATP Hydrolysis. An analysis of the RuvB ATPase activity in the presence of three different types of DNA is shown in Figure 4. Figure 4A and B demonstrate the effect of 100 μM circular or linear M13mp8 ssDNA, and Figure 4C and D show the effect of 100 μM linear duplex DNA derived from pJFS35r.

The data in Figure 4, panels A and B, show that the RuvB protein obeys Michaelis–Menten kinetics in the range of ATP concentration from 125 μM to 1 mM ATP when either circular or linear single-strand DNA is present in the reaction. As observed in the absence of DNA, the results at 3 mM ATP deviate somewhat from Michaelis–Menten kinetics, suggesting either a slight negative cooperativity or a titration of free magnesium by the ATP. These data provide a K_m for ATP of 145 ± 13 and 121 ± 10 μM ATP for conditions with circular and linear ssDNA, respectively (Table 1). The respective derived k_{cat} values are 5.87 ± 0.21 and 5.67 ± 0.17 min^{-1} . The rate at 3 mM ATP was again not included in the HYPER analysis of the data because of the apparent negative cooperativity. These data demonstrate that, within experimental error, single-stranded DNA has no significant effect on the steady-state parameters for RuvB protein-mediated ATP hydrolysis.

Panels C and D of Figure 4 show the effect of 100 μM linear double-strand pJFS35r DNA on the ATPase activity

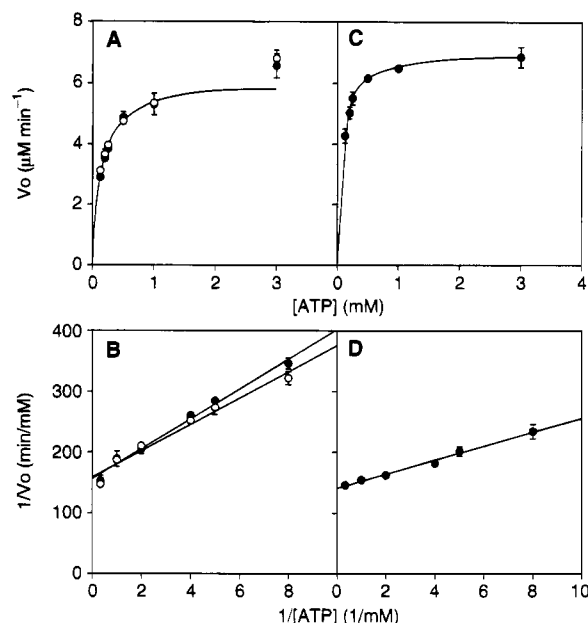


FIGURE 4: Steady-state kinetic analysis of RuvB-mediated ATP hydrolysis in the presence of ssDNA or linear dsDNA. Reactions were carried out as described in Materials and Methods and contained 1.05 μM RuvB protein and 100 μM of the indicated DNA. All data were obtained with the coupled spectrophotometric ATPase assay with substrate concentrations ranging from 125 μM to 3 mM ATP. Each data point is the average of three experiments performed on different days, and the error bars represent the range of data. (A and B) Reactions contained 100 μM circular (●) or linear (○) ssDNA. (C and D) Reactions contained 100 μM linear dsDNA (pJFS35r).

of the RuvB protein. Under these conditions, the ATPase activity obeys Michaelis–Menten kinetics over the entire substrate concentration range (125 μM to 3 mM ATP). These data provide a K_m value for ATP of 81 ± 9 μM ATP and a derived k_{cat} of 6.76 ± 0.24 min^{-1} (Table 1), indicating a modest effect of linear dsDNA on the observed kinetic parameters for ATP hydrolysis.

Slow Inactivation of RuvB-Mediated ATP Hydrolysis at an ATP Concentration near the K_m . The coupled spectrophotometric ATPase assay maintains the concentration of ATP at initial concentration throughout the assay (i.e., $[\text{ATP}] = [\text{ATP}]_0$). As a result, no ADP accumulation occurs in the reaction and the RuvB protein should hydrolyze ATP at a constant rate. We noted an unusual effect when concentrations of ATP were used that approximated the K_m for the reaction. Figure 5A shows a series of time courses for RuvB protein-mediated ATP hydrolysis at 125 μM ATP. The rate of ATP hydrolysis is approximately linear for ~10 min and then decreases until a negligible rate of ATP hydrolysis is observed after 30–40 min. These results were obtained with no DNA present in the reaction mixture and when either ssDNA or linear dsDNA was present at a concentration of 100 μM .

Controls were carried out to eliminate the trivial possibilities that the attenuation reflected either the removal of available ATP (e.g., by hydrolysis to AMP by an activity contaminating one of the reagents used) or a limitation of the spectrophotometer. To test for ATP degradation, α - ^{32}P -labeled ATP was added to reactions otherwise identical to those shown in Figure 5A. Aliquots removed after 25 min of reaction and analyzed by thin-layer chromatography showed that 99% of the label in the sample remained

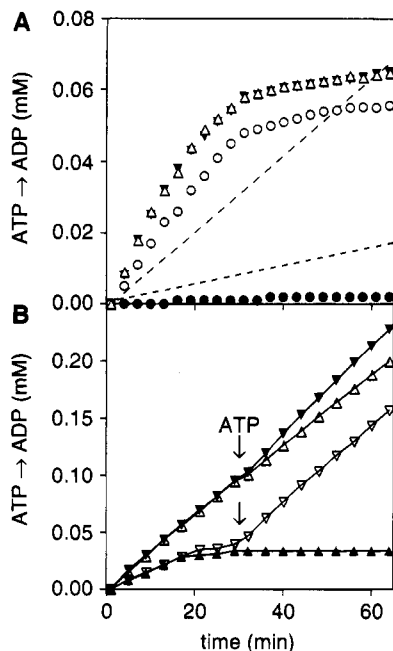


FIGURE 5: Attenuation of RuvB protein-mediated ATP hydrolysis. Reactions were carried out with the coupled spectrophotometric ATPase assay as described in Materials and Methods and contained (unless indicated) 1.05 μM RuvB protein and 125 μM ATP. Panel A shows the attenuation of ATP hydrolysis with time in the presence of no DNA (\circ), 100 μM circular ssDNA (Δ), or 100 μM linear dsDNA (\blacktriangledown ; pJFS35r). The line at the bottom (\bullet) shows a control reaction lacking RuvB protein and DNA. The dashed lines were selected from a series of control reactions with RuvB protein and supercoiled pJFS35r DNA concentrations adjusted to produce the rates shown. Although these controls also contain 125 μM ATP, the presence of the supercoiled DNA prevents attenuation (see Figure 9). These controls were done to confirm that the attenuation was not caused by equipment failure or equipment-introduced artifact. Panel B shows pairs of reactions carried out in the absence of DNA, with either 125 μM ATP (\blacktriangle , ∇) or 1 mM ATP (\blacktriangledown , \triangle). At 30 min (arrows), ATP was added to one reaction in each pair (\blacktriangledown , ∇), as described in Materials and Methods.

associated with ATP. An additional series of control reactions were carried out to test the capacity of the coupling system and the spectrophotometer to monitor rates of RuvB-mediated ATP hydrolysis that are equal to or lower than the rates observed prior to attenuation. Reactions with RuvB and supercoiled pJFS35r DNA concentrations adjusted to produce the lower rates exhibit a linear production of ADP for at least 80 min, demonstrating that the attenuation is not an artifact of the equipment or conditions used (Figure 5A).

The attenuation effect was observed in 15 separate trials carried out under the indicated conditions, some of them done with a second preparation of RuvB protein. This is not a single-turnover phenomenon. In experiments carried out under the conditions in Figure 5A, ~ 60 ATPs are hydrolyzed per RuvB monomer before the maximum attenuation is observed.

The experiment presented in Figure 5B demonstrates the attenuation of the RuvB ATPase can be reversed by the addition of ATP. This experiment demonstrates that the attenuation of the ATPase activity does not reflect an irreversible inactivation. Addition of ATP to a final concentration of 3 mM results in a resumption of ATP hydrolysis with no evident lag, and the final rate of ATP hydrolysis (roughly 6 $\mu\text{M}/\text{min}$) is comparable to reactions in which the ATP was present at 3 mM from the beginning.

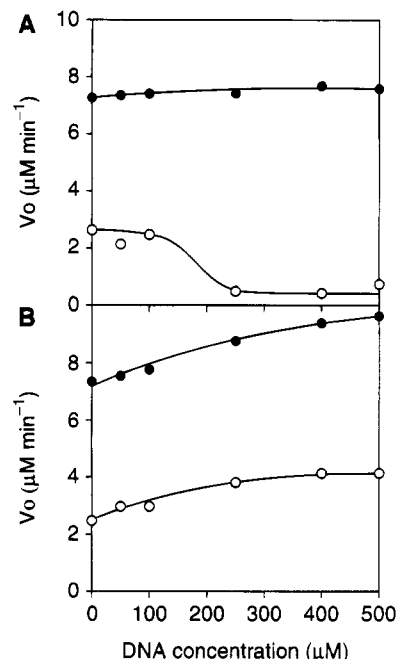


FIGURE 6: Effects of DNA concentration on RuvB protein-mediated ATP hydrolysis. Reactions were carried out as described in Materials and Methods, with 1.05 μM RuvB protein and either 125 μM (\circ) or 3 mM (\bullet) ATP. Panels A and B show the effects of circular ssDNA (M13mp8) or linear dsDNA (pJFS35r), respectively.

Effect of Circular M13mp8 ssDNA and Linear pJFS35r dsDNA Concentration on the RuvB Protein ATPase Activity at 125 μM and 3 mM ATP. These experiments are designed to determine whether there is any effect of higher concentrations of single-stranded M13mp8 DNA or linear duplex pJFS35r DNA on the observed rates of RuvB protein-mediated ATP hydrolysis. Figure 6A shows the effect of varying circular ssDNA concentration at 125 μM and 3 mM ATP. At 3 mM ATP, the increase in DNA concentration had no significant effect on the observed rates of ATP hydrolysis. In contrast, at 125 μM ATP, the increase in M13mp8 ssDNA concentration had a pronounced inhibitory effect on the observed rate of ATP hydrolysis by the RuvB protein. In reactions from 0 to 100 μM total DNA, the ATP hydrolysis rate was relatively constant at 2.3 $\mu\text{M}/\text{min}$, but when DNA concentration exceeded 250 μM , the rate of ATP hydrolysis dropped to 0.4 $\mu\text{M}/\text{min}$. This rate of ATP hydrolysis is at the detection limit of the coupled spectrophotometric ATPase assay.

Figure 6B shows the effect of linear double-strand pJFS35r DNA concentration on the observed rates of ATP hydrolysis by the RuvB protein at 125 μM and 3 mM ATP. A similar small increase in ATP hydrolysis rates is seen at both ATP concentrations as the DNA concentration increases. The attenuation of RuvB ATPase activity at 125 μM ATP (Figure 5) is still present at all linear dsDNA concentrations examined (data not shown).

Effects of Circular dsDNA on the RuvB Protein ATPase Activity. Results obtained with circular duplex DNA as a cofactor for ATP hydrolysis were dramatically different. Figure 7 illustrates the effect of circular dsDNA on the RuvB protein ATPase activity. The effects of supercoiled DNA are seen in Figure 7A,B. As the substrate concentration increases from 50 to 500 μM ATP, there is a corresponding increase in the rate of ATP hydrolysis. However as the ATP concentration increases from 1 to 5 mM ATP, the initial rates

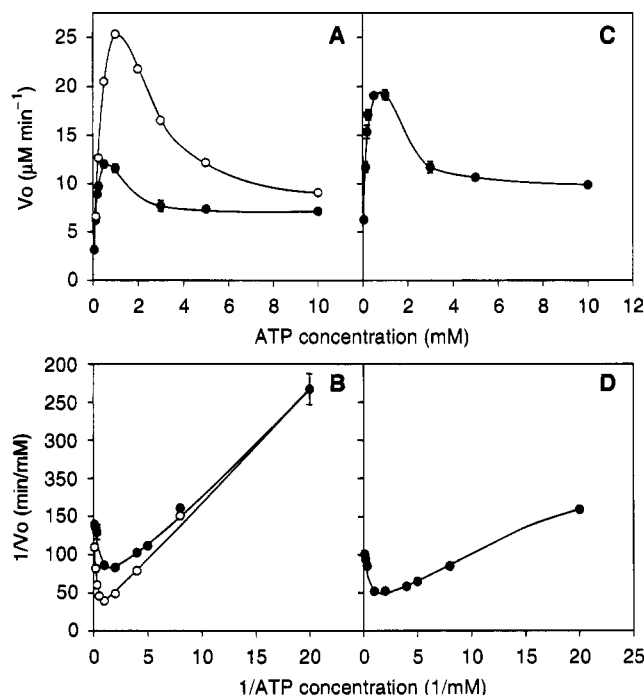


FIGURE 7: Steady-state kinetic analysis of RuvB protein-mediated ATP hydrolysis in the presence of circular dsDNA. Reactions were carried out as described in Materials and Methods with $1.05 \mu\text{M}$ RuvB protein. (A and B) Reactions with supercoiled dsDNA (pJFS35r), at a concentration of $100 \mu\text{M}$ (●) or $500 \mu\text{M}$ (○). (C and D) Reactions with $100 \mu\text{M}$ relaxed dsDNA (pJFS35r). For all reactions with $100 \mu\text{M}$ DNA, each data point is the average of three experiments performed on different days and error bars are the range of the data. For the reactions with $500 \mu\text{M}$ supercoiled dsDNA in panels A and B, two separate experiments are shown at each ATP concentration. Lines drawn through the data in panels B and D are approximate and are not fitted to any data analysis program.

of ATP hydrolysis decrease with increasing ATP concentration (Figure 7A), reflecting substrate inhibition (Cleland, 1979b). The rates level off at the highest ATP concentrations (5 and 10 mM), showing that the substrate inhibition is partial rather than total. Because of the complexities involved in analyzing partial substrate inhibition (Cleland, 1979b), no effort was made to derive extrapolated steady-state kinetic parameters from these data. However, as compared to reactions with no DNA, ssDNA, or linear dsDNA, the supercoiled DNA provides a large stimulation of the ATPase activity. A maximal level of ATPase activity occurs between 0.5 and 1 mM ATP, where the measured turnover is 2–4 times greater than the derived k_{cat} values reported for other conditions in Table 1. The effects were not dependent on a particular protein preparation or the size of the plasmid DNA (data not shown).

Similar experiments were carried out with $100 \mu\text{M}$ circular dsDNA that had been relaxed with topoisomerase I (Figure 7C,D). The partial substrate inhibition effect is still evident. Qualitatively, the effect is similar to that observed for reactions with supercoiled pJFS35r DNA, although the measured rates of ATP hydrolysis at any given ATP concentration were 1.5–2-fold higher than those measured in the presence of $100 \mu\text{M}$ supercoiled DNA (compare panels B and D in Figure 7).

The effect of the concentration of circular dsDNA on ATP hydrolysis at a constant concentration of ATP is shown in Figure 8. A pronounced increase in ATP hydrolysis rates

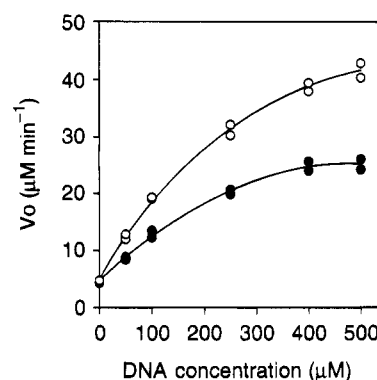


FIGURE 8: Effect of circular dsDNA concentration on the rate of RuvB protein-mediated ATP hydrolysis. Reaction conditions and cofactors were as in Figure 7, and 1 mM ATP. The effects of supercoiled (●) or relaxed (○) DNA are shown.

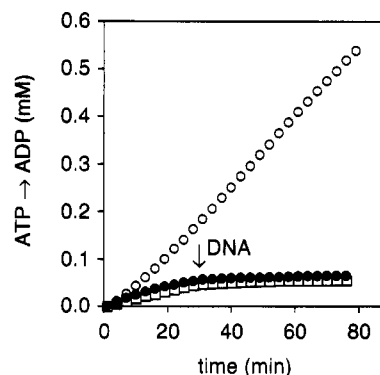


FIGURE 9: Effects of circular dsDNA on the attenuation of RuvB-mediated ATP hydrolysis seen at $125 \mu\text{M}$ ATP. Reactions were carried out as described in Materials and Methods and in the legend to Figure 5 and contained $1.05 \mu\text{M}$ RuvB protein and $125 \mu\text{M}$ ATP. The individual reactions contained the following: (□) no addition; (●) $100 \mu\text{M}$ supercoiled dsDNA (pJFS35r) added at 30 min (arrow); (○) $100 \mu\text{M}$ supercoiled dsDNA added at time zero.

is observed that appears to level off at or near $400 \mu\text{M}$ DNA. The topoisomerase I-relaxed pJFS35r DNA titrations do not show as definitive an end point as the supercoiled DNA. At the highest DNA concentration ($500 \mu\text{M}$) nucleotides, the actual concentration of DNA is 178 nM in molecules, and the concentration of RuvB hexamers (assuming all the RuvB is in the hexameric form) is 158 nM . This suggests that the leveling off of the rate coincides with the presence of at least one DNA circle for each RuvB hexamer on average.

The time-dependent attenuation of ATPase activity, in reactions with a substrate concentration of $125 \mu\text{M}$ ATP (see Figure 5), was not observed when 100 or $500 \mu\text{M}$ supercoiled DNA, or $100 \mu\text{M}$ relaxed circular dsDNA, was present (Figure 9 and data not shown). If supercoiled DNA had been added to a reaction in which ATP hydrolysis had been attenuated, the ATPase activity was not restored (Figure 9).

Lag in RuvB-Mediated ATP Hydrolysis in the Presence of Circular dsDNA. There is a lag of approximately 8–10 min observed in reactions with circular dsDNA before the reactions exhibit a linear rate of ATP hydrolysis (Figure 10A). The system lag for the coupling system (a delay during which the activities of the coupling components reach steady state) is only 1–2 min in these experiments, and a lag longer than 1–2 min is not observed in experiments with no DNA, ssDNA, or linear dsDNA (Figures 5 and 10 and data not shown). The effect is therefore unique to circular dsDNA and is seen in all reactions with supercoiled or

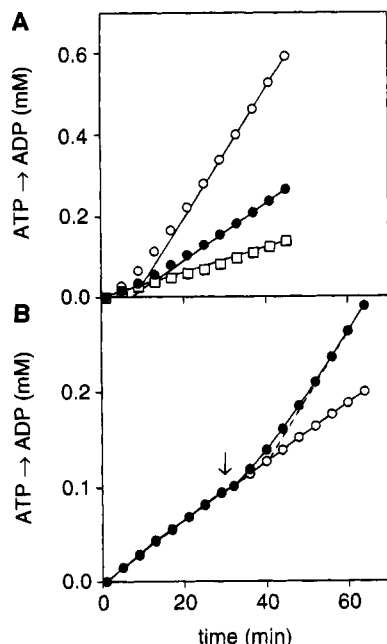


FIGURE 10: Effects of supercoiled dsDNA on RuvB protein-mediated ATP hydrolysis. Reactions contained 1.05 μ M RuvB protein and 1 mM ATP and were carried out as described in Materials and Methods. (A) Reactions contained the following: (\square) no DNA; (\bullet) 100 μ M supercoiled DNA; (\circ) 500 μ M supercoiled DNA. (B) reactions contained the following: (\circ) no DNA; (\bullet) 100 μ M supercoiled dsDNA added at 30 min (arrow).

relaxed DNA at ATP concentrations of 125 μ M to 3 mM (data not shown). The lag time in experiments with an 18 kbp plasmid was still 10 min (data not shown). These results indicate that the lag is not dependent on DNA concentration or DNA length. The lag was shortened when ATP concentrations of 5 or 10 mM were used (data not shown).

To determine whether the lag reflected a change in the RuvB protein (e.g., a conformation change required to bind to circular DNA), as opposed to an assembly process on the DNA, we determined whether incubation of RuvB protein with ATP prior to DNA addition affected the lag. An ATPase assay (1 mM ATP) was started by the addition of RuvB protein and allowed to react for 30 min without DNA. Supercoiled pJFS35r plasmid DNA was then added to the reaction in buffer B to 100 μ M, and the reaction was followed for an additional 35 min. After the addition of the supercoiled DNA, there was once again a lag of \sim 10 min before the ATP hydrolysis rate became linear (Figure 10B). A final rate of ATP hydrolysis of 11.2 μ M/min was obtained from the linear portion of the curve. This rate is comparable to rates obtained when 100 μ M supercoiled pJFS35r DNA was present in the reactions mixture from the beginning of the reaction (11.6 μ M/min; data not shown).

A Burst in RuvB-Mediated ATP Hydrolysis. To examine a single turnover in the ATP hydrolytic reaction, the RuvB protein concentration was increased and the ATP concentration was decreased, and reactions were monitored by the TLC assay. In Figure 11A–C, a burst in ATP hydrolysis is seen with no DNA and in the presence of either ssDNA or supercoiled DNA. In all reactions, RuvB protein concentration ranged from 5.25 to 21 μ M in monomers. The burst size (μ M ATP) is plotted versus RuvB protein monomer concentration in Figure 11D–F. Lines fitted to these data give a ratio of RuvB monomers to ATP molecules of 3.3

(\pm 0.2):1, 3.2 (\pm 0.1):1, and 3.1 (\pm 0.2):1, for no DNA, 100 μ M circular M13mp8 ssDNA, and 100 μ M supercoiled pJFS35r DNA, respectively. The calculated burst size represents the mean of the eight independent determinations shown in each panel, with the error reported as the standard error of the mean. The data are consistent with a burst of ATP hydrolysis corresponding to 1 ATP to 3 RuvB protomers. Given the lag described in Figure 10 in the ATPase reaction with supercoiled DNA, it is unlikely that the supercoiled DNA present in some of these experiments has much effect on the data over this time course. The same seems to be true of the ssDNA present in one set of experiments.

The results in Figure 11 were obtained with ATP concentrations below the measured K_m for ATP (see Table 1). The conditions chosen reflected technical limitations imposed by the TLC assay we used, which measures ATP hydrolysis in terms of the fraction of the total converted to ADP. At ATP concentrations on the order of 1 mM, the fraction of the total ATP converted to ADP during a burst phase by any achievable concentration of RuvB would be much too small to measure accurately. At substrate concentrations below K_m , there is generally either no burst or the observed burst is proportional to the substrate concentration (Fersht, 1985). The burst we observe does not change appreciably when the ATP concentration is varied. This can be seen in Figure 11, in which the reactions in panels A and B reflect different ATP concentrations but the derived K_m s for the two situations (no DNA or with ssDNA) are similar (Table 1). Additional pairs of experiments were carried out with 25 or 50 μ M ATP in parallel (data not shown). Under conditions otherwise identical to those in Figure 11C, a burst of 1 ATP/3.2 RuvB monomers was observed at 25 μ M ATP, with 1 ATP/3.3 monomers of RuvB observed at 50 μ M ATP. Identical results were obtained in a similar pair of experiments carried out under the conditions of Figure 11A.

DISCUSSION

RuvB protein-mediated ATP hydrolysis has the following characteristics: (a) A substantial activity is observed in the absence of DNA, exhibiting ATP turnover rates approaching 6 min^{-1} . The DNA-independent activity requires an apparent critical concentration of \sim 200 nM RuvB protein. This ATP hydrolytic activity is only moderately affected by ssDNA or linear dsDNA. (b) A substantial stimulation of ATP hydrolysis is brought about by circular dsDNA. The circular dsDNA-dependent reaction is subject to strong substrate inhibition. There is an 8–10 min lag observed before maximum rates of ATP hydrolysis on circular dsDNA are achieved. (c) At lower ATP concentrations, the ATP hydrolytic activity is severely attenuated unless circular dsDNA is present. (d) Rates of circular dsDNA-stimulated ATP hydrolysis peak only when the concentration of available DNA circles exceeds that of RuvB hexamers. (e) There is a burst of ATP hydrolysis observed under all conditions that corresponds to \sim 1 ATP hydrolyzed per 3 RuvB monomers. As described in more detail below, we interpret observations b–e within the context of a dynamic RuvB hexamer that translocates on dsDNA and possesses nonequivalent ATP hydrolytic sites. This survey is intended to facilitate more detailed investigations of the ATP hydrolytic activity of RuvB.

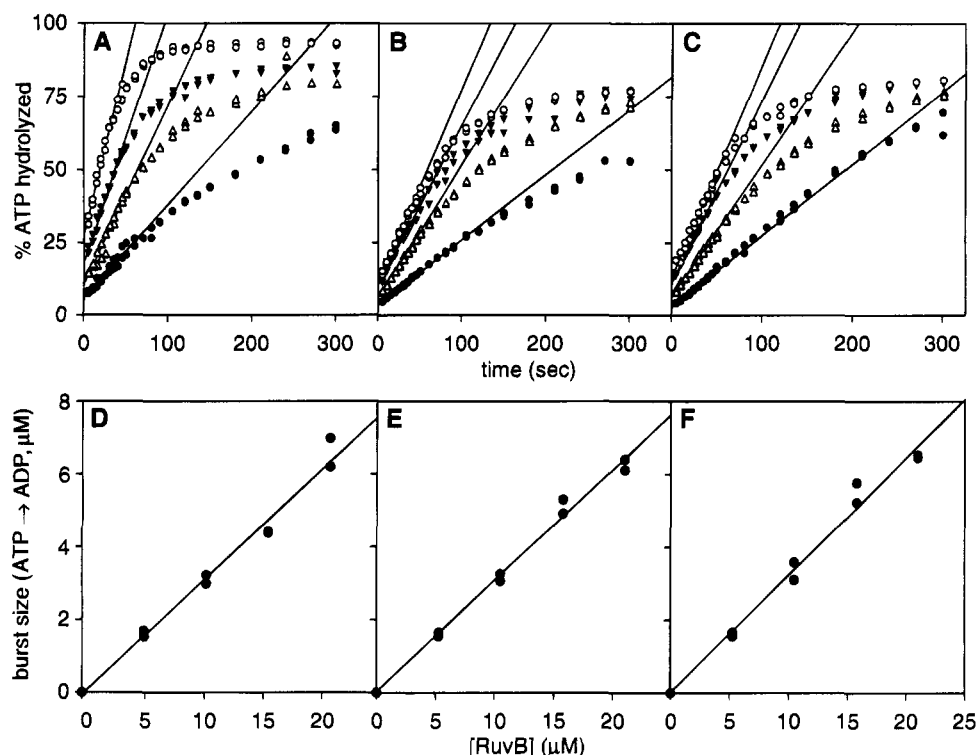


FIGURE 11: Burst in ATP hydrolysis under pre-steady-state conditions. Reactions were carried out with the TLC assay as described in Materials and Methods: (A and D) reactions with no DNA and 25 μM ATP; (B and E) reactions with 100 μM circular ssDNA and 50 μM ATP; (C and F) reactions with 100 μM supercoiled dsDNA and 50 μM ATP. In the four reactions in each of the top three panels (A–C), RuvB protein concentrations were 5.25, 10.5, 15.75, and 21 μM from bottom to top, respectively. Data from two independent reactions are shown in each case. Data for burst size in panels D–F was calculated as described in Materials and Methods.

The modest effects of ssDNA and linear dsDNA on the ATP hydrolytic activity do not mean that there is no interaction of RuvB with these substrates. High concentrations of ssDNA have a strong inhibitory effect on the ATP hydrolytic activity with low concentrations of ATP (Figure 6). Somewhat greater stimulatory effects of linear dsDNA have been reported, with the effects increasing with DNA length (Mitchell & West, 1994).

The stimulation of ATP hydrolysis by circular dsDNA has been reported previously (Mitchell & West, 1994). This effect is characterized here in detail to reveal a strong substrate inhibition and a lag in the ATP hydrolysis reaction. The length of the lag exhibits no apparent dependence on DNA concentration, DNA molecule size, or extended pre-incubation of RuvB and ATP in the absence of DNA. The lag is decreased in the presence of ATP concentrations higher than 3 mM. The lag may be caused by an activation or assembly step after an initial RuvB encounter with circular dsDNA. We did not observe the positive cooperativity in ATP hydrolytic rates reported by Mitchell and West (1994) in reactions containing circular duplex DNA. The curvature in their double-reciprocal plots may instead reflect the substrate inhibition we characterize in Figure 7.

West and colleagues have advanced the notion that RuvB translocates on the DNA and have provided evidence that the active species is a hexamer under the conditions used in the current study (Mitchell & West, 1994). For DNA helicase II, an increase in ATP hydrolysis with increasing DNA length has been interpreted as evidence for translocation on the DNA (Matson & George, 1987). Young et al. (1994a,b) have expanded this treatment of translocating ATPases to a general theory for how the rate of ATP hydrolysis should increase with the length of DNA. If the

circular DNA is considered to be a duplex DNA of infinite length, the dramatic stimulation of ATP hydrolysis with the circular duplexes can then be interpreted by the criteria of Young et al. (1994a,b) as evidence for the translocation of RuvB on DNA. Also, there is an apparent saturation of circular dsDNA-dependent ATP hydrolysis when the concentration of DNA circles exceeds the concentration of RuvB hexamers (Figure 8). This suggests that multiple hexamers on a circle interfere with each other, as might occur if the hexamers translocated on the DNA. West and colleagues (Parsons et al., 1995) have recently described an interesting model by which a translocation function of RuvB can be utilized at a DNA branch in conjunction with RuvA to effect branch migration.

There are several new results which suggest that the presumed six ATP hydrolytic sites in a RuvB hexamer are nonequivalent. First, when ATP concentrations approximate the K_m for ATP hydrolysis, there is an attenuation of ATP hydrolysis with time unless circular dsDNA is present. This may reflect an inactive conformation, a disassembly of the hexamer, or perhaps the association of two hexamers to form an inactive dodecamer. The attenuation is readily reversible with the addition of more ATP (Figure 5) but is not affected by addition of circular dsDNA (Figure 9). Perhaps the occupancy of the wrong subset of the hexamer's hydrolytic sites can trigger a conversion to a less active RuvB species. Second, the strong substrate inhibition observed on circular dsDNA can be interpreted as reflecting part-of-the-sites reactivity. The substrate inhibition observed with RuvB is unusual in that it is seen at physiological concentrations of ATP (Cleland, 1979b). Finally, the burst of ATP hydrolysis observed under single-turnover conditions shows that 1 ATP is hydrolyzed per 3 RuvB monomers in a rapid phase. The

first two of these results are subject to alternative interpretations but, when combined with the burst results, are readily explained within the context of nonequivalent ATP binding sites.

The burst is potentially informative. Since the functional unit of RuvB protein for ATPase activity appears to be a hexamer of RuvB protein protomers (Mitchell and West, 1994), the burst corresponds to 2 ATP molecules hydrolyzed per hexamer. Although for technical reasons we measured the burst at ATP concentrations below the derived K_m for ATP, the magnitude of the burst exhibited little dependence on ATP concentration. This suggests that the burst reflects the two ATP binding sites in the hexamer with the highest affinity for ATP. The derived K_m may reflect the interaction of ATP with other (lower affinity) ATP binding sites in the hexamer.

The burst may reflect the functional organization of the hexamer. Hydrolysis of ATP in two subunits of the hexamer may activate ATP hydrolysis in other subunits, with different promoter pairs hydrolyzing ATP in a sequential manner. Alternatively, the hexamer may be functionally and/or structurally asymmetric, with two subunits possessing ATP hydrolytic sites with a higher affinity for ATP. The burst could further reflect a functional organization of the hexamer as a dimer of trimers. The latter idea would distinguish RuvB from some other hexameric helicases. Rho protein has been shown to function as a trimer of dimers (Geiselman et al., 1993; Seifried et al., 1992).

We note that in the course of efforts to detect unwinding of circular dsDNA by RuvB, West and colleagues (Adams & West, 1995) found that a significant degree of unwinding was stabilized in the presence of mixtures of ATP and ATP γ S, with an optimal ratio of 1 ATP to 2 ATP γ S molecules. This ratio corresponds to 2 ATP molecules and 4 ATP γ S molecules per hexamer (on average) and could be related to the burst observed in the current study.

ACKNOWLEDGMENT

We thank W. Wallace Cleland for suggestions on computer programs and methods for data analysis, and Gwendolyn Sowa for help with using the computer programs. We also thank Timothy Lohman and W. Wallace Cleland for critical readings of the manuscript that produced many useful suggestions.

REFERENCES

- Adams, D. E., & West, S. C. (1995) *J. Mol. Biol.* 247, 404–17.
- Benson, F. E., Illing, G. T., Sharpless, G. J., & Lloyd, R. G. (1988) *Nucleic Acids Res.* 16, 1541–9.
- Bujalowski, W., Klonowska, M. M., & Jezewska, M. J. (1994) *J. Biol. Chem.* 269, 31350–8.
- Cleland, W. W. (1979a) *Methods Enzymol.* 63, 103–38.
- Cleland, W. W. (1979b) *Methods Enzymol.* 63, 500–13.
- Davis, R. W., Botstein, D., & Roth, J. R. (1980) *Advanced Bacterial Genetics*, Cold Spring Harbor Laboratory, Cold Spring Harbor, NY.
- Dean, F. B., & Hurwitz, J. (1991) *J. Biol. Chem.* 266, 5062–71.
- Dean, F. B., Borowiec, J. A., Eki, T., & Hurwitz, J. (1992) *J. Biol. Chem.* 267, 14129–37.
- Edelhoc, H. (1948) *Biochemistry* 6, 1948–54.
- Fersht, A. (1985) *Enzyme Structure and Mechanism*, pp 143–7, W. H. Freeman & Co., New York.
- Geiselman, J., Seifried, S. E., Yager, T. D., Liang, C., & von Hippel, H. P. (1992a) *Biochemistry* 31, 121–32.
- Geiselman, J., Yager, T. D., Gill, S. C., Calmettes, P., & von Hippel, H. P. (1992b) *Biochemistry* 31, 111–21.
- Geiselman, J., Yager, T. D., & von Hippel, H. P. (1992c) *Protein Sci.* 1, 861–73.
- Geiselman, J., Wang, Y., Seifried, S. E., & von Hippel, H. P. (1993) *Proc. Natl. Acad. Sci. U.S.A.* 90, 7754–8.
- Gill, S. C., & von Hippel, H. P. (1989) *Anal. Biochem.* 182, 319–26.
- Iwasaki, H., Shiba, T., Makino, K., Nakata, A., & Shinagawa, H. (1989) *J. Bacteriol.* 171, 5276–80.
- Iype, L. E., Wood, E. A., Inman, R. B., & Cox, M. M. (1994) *J. Biol. Chem.* 269, 24967–78.
- Iype, L. E., Inman, R. B., & Cox, M. M. (1995) *J. Biol. Chem.* (submitted).
- Kowalczykowski, S. C., Dixon, D. A., Eggleston, A. K., Lauder, S. D., & Rehauer, W. M. (1994) *Microbiol. Rev.* 58, 401–65.
- Kuzminov, A. (1993) *Bioessays* 15, 355–8.
- Lindsley, J. E., & Cox, M. M. (1990) *J. Biol. Chem.* 265, 9043–54.
- Lloyd, R. G., & Sharpless, G. J. (1993) *Nucleic Acids Res.* 21, 1719–25.
- Lohman, T. M. (1992) *Mol. Microbiol.* 6, 5–14.
- Lohman, T. M. (1993) *J. Biol. Chem.* 268, 2269–72.
- Lohman, T. M., Chao, K., Green, J. M., Sage, S., & Runyon, G. T. (1989) *J. Biol. Chem.* 264, 10139–47.
- Matson, S. W., & George, J. W. (1987) *J. Biol. Chem.* 262, 2066–76.
- Messing, J. (1983) *Methods Enzymol.* 101, 20–78.
- Mitchell, A. H., & West, S. C. (1994) *J. Mol. Biol.* 243, 208–15.
- Moore, K. J. M., & Lohman, T. M. (1994) *Biochemistry* 33, 14550–64.
- Morrill, S. W., Lee, J., & Cox, M. M. (1986) *Biochemistry* 25, 1482–94.
- Müller, B., & West, S. C. (1994) *Experientia* 50, 216–22.
- Neuendorf, S. K., & Cox, M. M. (1986) *J. Biol. Chem.* 261, 8276–82.
- Parsons, C. A., Stasiak, A., Bennett, R. J., & West, S. C. (1995) *Nature* 374, 375–8.
- Seifried, S. E., Easton, J. B., & von Hippel, H. P. (1992) *Proc. Natl. Acad. Sci. U.S.A.* 89, 10454–8.
- Senecoff, J. F., & Cox, M. M. (1986) *J. Biol. Chem.* 261, 7380–6.
- Shinagawa, H., Makino, K., Amemura, M., Kimura, S., Iwasaki, H., & Nakata, A. (1988) *J. Bacteriol.* 170, 4322–9.
- Shinagawa, H., Shiba, T., Iwasaki, H., Makino, K., Takahagi, M., & Nakata, A. (1991) *Biochimie* 73, 505–7.
- Stasiak, A., Tsaneva, I. R., West, S. C., Benson, C. J., Yu, X., & Egelman, E. H. (1994) *Proc. Natl. Acad. Sci. U.S.A.* 91, 7618–22.
- Tsaneva, I. R., & West, S. C. (1994) *J. Biol. Chem.* 269, 26552–8.
- Tsaneva, I. R., Illing, G., Lloyd, R. G., & West, S. C. (1992a) *Mol. Gen. Genet.* 235, 1–10.
- Tsaneva, I. R., Müller, B., & West, S. C. (1992b) *Cell* 69, 1171–80.
- Tsaneva, I. R., Müller, B., & West, S. C. (1993) *Proc. Natl. Acad. Sci. U.S.A.* 90, 1315–9.
- Wang, Y., & von Hippel, H. P. (1993) *J. Biol. Chem.* 268, 13947–55.
- West, S. C., & Connolly, B. (1992) *Mol. Microbiol.* 6, 2755–9.
- West, S. C., Tsaneva, I. R., Hiom, K., & Benson, F. E. (1993) *Cold Spring Harbor Symp. Quant. Biol.* 58, 525–31.
- Wong, I., & Lohman, T. M. (1992) *Science* 256, 350–5.
- Wong, I., Chao, K. L., Bujalowski, W., & Lohman, T. M. (1992) *J. Biol. Chem.* 267, 7596–610.
- Young, M. C., Kuhl, S. B., & von Hippel, H. P. (1994a) *J. Mol. Biol.* 235, 1436–46.
- Young, M. C., Schultz, D. E., Ring, D., & von Hippel, H. P. (1994b) *J. Mol. Biol.* 235, 1447–58.